Studies by the U.S. Geological Survey in Alaska, 2001
U.S. Geological Survey Professional Paper 1678

Geology and Late Quaternary Eruptive History of Kanaga Volcano, a Calc-Alkaline Stratovolcano in the Western Aleutian Islands, Alaska

By Christopher F. Waythomas, Thomas P. Miller, and Christopher J. Nye

Abstract

Recent studies of the geology and eruptive history of Kanaga Volcano in the western Aleutian Islands of Alaska have yielded new information about the timing of Holocene eruptions and an improved understanding of the evolution of the volcano. Previous studies indicated that Kanaton Ridge, a major topographic feature on the northern part of Kanaga Island, was the rim of a collapse caldera. Our studies indicate that the caldera structure more likely formed as the result of a northward-directed flank collapse that was not necessarily associated with a major eruption. Dacitic lapilli tephra deposits began accumulating on Kanaga Island about 11 ka, and we infer that most of the modern volcanic cone developed in Holocene time. At least 11 major tephra-producing eruptions of Kanaga Volcano have been documented since about 11 ka, in addition to known historical eruptions in 1763, 1768, 1786, 1790, 1791, 1827, 1829, 1904, 1906, and 1993–95. Tephra deposits on nearby Adak Island were believed to have been erupted from Kanaga Volcano throughout the Holocene. Our tephrostratigraphic and chronologic data indicate that only a few of these tephra deposits can be directly correlated with eruptions of Kanaga Volcano, and so the source of the major pumiceous tephra deposits on Adak Island is uncertain. Holocene eruptions of Mount Moffett, a broad composite cone on the northern part of Adak Island, now appears to be a possible source volcano for many of the tephra deposits on Adak Island.

Introduction

Since 1996, the Alaska Volcano Observatory has been systematically expanding its volcano-monitoring program and, at the same time, initiating new studies of the geology, eruptive history, and hazards of several active volcanoes in the Aleutian Arc of Alaska. Many volcanoes in this region have never been studied in detail; geologic maps are preliminary at best, and information about Holocene eruptions is generally unknown. Although the Aleutian Islands are a remote area inhabited by few people, eruptions from this region pose substantial hazards to overflying jet aircraft traveling North Pacific air routes between North America and the Far East. Projected increases in air travel over this region have heightened concern about the potential hazard to jet aircraft from explosively generated plumes of volcanic ash. Recent studies by the Alaska Volcano Observatory have been focused on addressing this concern by studying the geology and eruptive history of historically active volcanoes in the Aleutian Arc to better understand the characteristics of future explosive eruptions. Here, we report results from our study of Kanaga Volcano, an active calc-alkaline stratovolcano in the western Aleutian Islands of Alaska (fig. 1).

Kanaga Volcano is a 1,300-m-high, cone-shaped andesitic stratovolcano on the north end of Kanaga Island (lat 51°55′ N., long 177°10′ W.) in the Andreanof Islands Group of the western Aleutian Islands (fig. 1). The volcano is about 30 km west of Adak Island and the community of Adak, the site of a former U.S. Naval installation that still supports a major airfield and serves as an alternative landing site for trans-Pacific aircraft. Kanaga Volcano has erupted numerous times in the past 10 k.y., including at least 10 Strombolian-type to sub-Plinian eruptions in the past 250 years (Miller and others, 1998). The most recent eruption, in 1993–95, produced several aa lava flows that descended the northwest flank of the volcano to the sea (fig. 2), and several small-volume, low-altitude plumes of volcanic ash that at least once drifted eastward over Adak Island and deposited a few millimeters of fine ash on the northern part of Adak Island.

Kanaga Volcano is undissected, symmetrical in profile, and characterized by numerous blocky lava flows, with well-developed levees and steep flow fronts, that descend radially from or near the 200-m-wide summit vent crater (fig. 2). The flanks of the cone are steep (25°–30°) and consist of blocky aa lava flows, talus, spatter, coarse tephra, and clast-rich lahar deposits. The volcano does not support glaciers but is snow covered almost year round. The cone itself shows little evidence of dissection by streams or glaciers and so could have been entirely constructed in postglacial Holocene time. The volcano is one of the more active Aleutian volcanoes, and historical eruptions were reported in 1791, 1827, 1829, 1904,

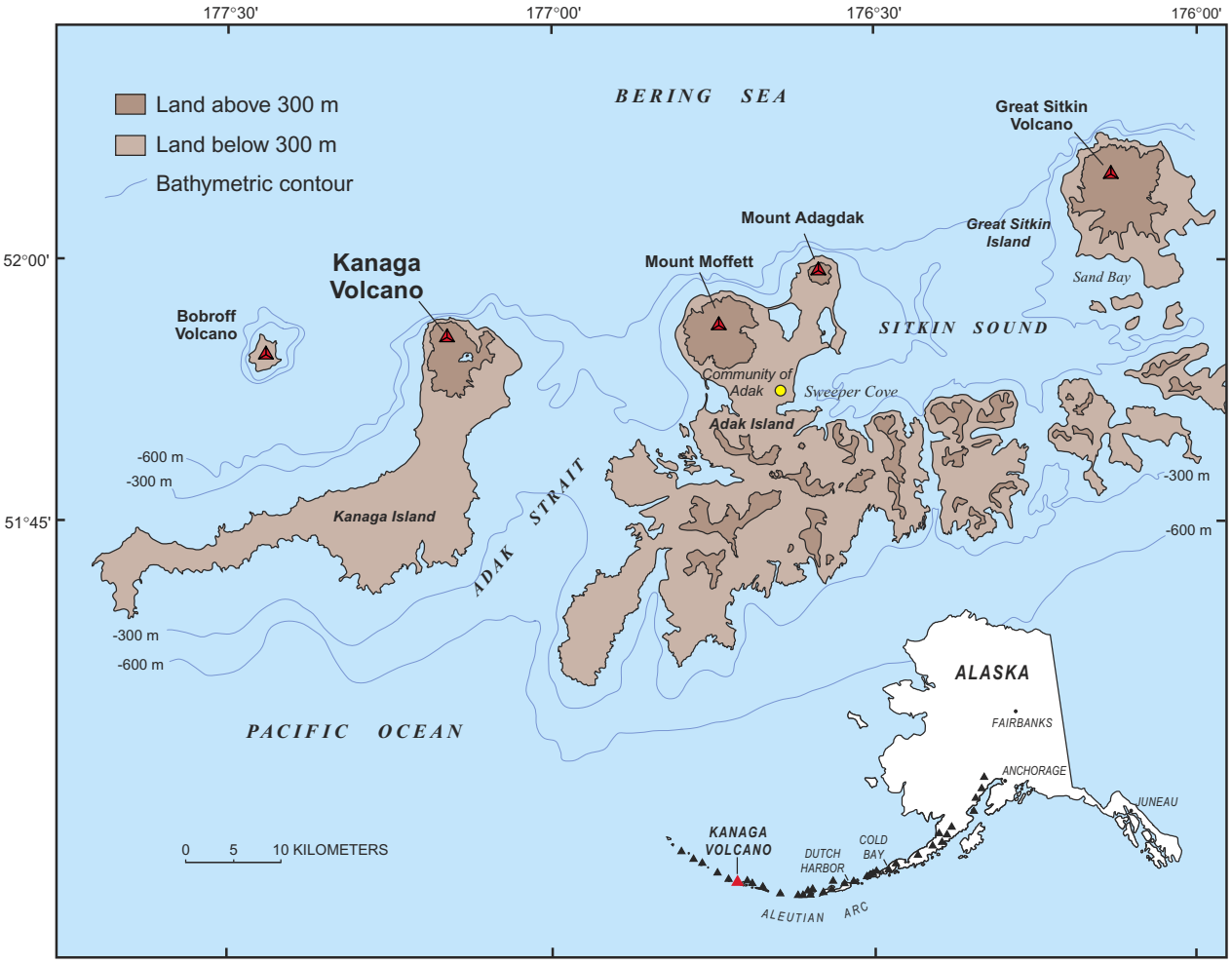

Figure 1. Western part of the Aleutian Islands, Alaska, showing location of Kanaga Volcano.

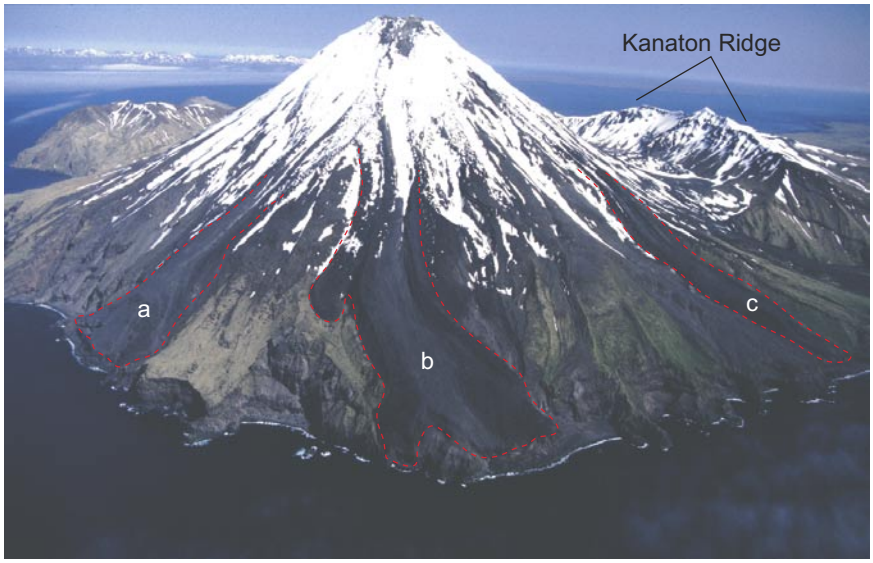

Figure 2. Kanaga Volcano. Areas a through e (outlined with red dashed line), blocky aa lava flow erupted during 1993–95. Kanaton Ridge is in background. Summit altitude, 1,307 m. View southeastward; photograph by C.J. Nye, Alaska Division of Geological and Geophysical Surveys, taken July 2000.

and 1993–95 (Miller and others, 1998); less well documented eruptions also were reported in 1763, 1768, 1786, 1790, and 1933.

The geology of the northern part of Kanaga Island was studied briefly in 1946 by R.R. Coats, who produced the first known geologic map of Kanaga Volcano based on about 10 days of fieldwork on foot (Coats, 1956). Coats described most of the major lithologic units on the northern part of Kanaga Island and made several important observations about the geology of Kanaga Volcano. He recognized Mount Kanaton, an ancestral volcano part surrounding the modern Kanaga cone, and inferred that Mount Kanaton was destroyed by structural collapse which he believed during a caldera-forming eruption. Coats also identified several older eruptive centers on the flanks of ancestral Mount Kanaton (Coats, 1956).

More recent investigations of the geology of the northern part of Kanaga Island have been petrologic studies of basaltic lava flows on Kanaton Ridge (Brophy, 1989, 1990) and at Round Head (Whittington, 1996). We visited Kanaga Island during June and July 1999 and 2000 and refined the geologic map of the volcano, sampled major lithologic units and other deposits, and evaluated the hazards posed by future eruptions. We also investigated the record of Holocene eruptive activity by studying and sampling tephra deposits in shallow stratigraphic exposures on the flanks of Mount Kanaton and Kanaga Volcano. Previous work on nearby Adak Island (Black, 1980; Romick and others, 1992; Kiriyanov and Miller, 1997), where multiple beds of pumiceous lapilli tephra of Holocene age are preserved, attributed several of these tephra deposits to eruptions of Kanaga Volcano. We thus sought to evaluate the origin of the tephra deposits on Adak Island to determine whether Kanaga Volcano was indeed the source.

Geology of the Volcano

The focus of our studies was the modern cone of Kanaga Volcano and its associated deposits. We spent little time mapping and sampling the older rocks and deposits that were described by Coats (1956). To give a better overall synopsis of the volcano, we include a brief summary of the geology of these older volcanic rocks.

Older Volcanic Cones

Kanaga Volcano is partly surrounded by, and in fault contact with, at least three overlapping volcanic cones older than the present edifice, including two small composite cones on the northeast coast of the island and a shield like edifice called Mount Kanaton by Coats (1956). The oldest of the three cones, which is exposed along the northeast coast of the island immediately east of Kanaga Volcano (fig. 3; Coats, 1956; Brophy, 1990), consists mainly of thick-bedded to massive basaltic and andesitic lava flows and includes a few beds of volcanic breccia and tuff. Most of the rocks in the cone are hydrothermally altered, and as a result, small debris-avalanche and landslide deposits are common on the flanking slopes.

The second cone is a small satellite eruptive center on the northeast side of Kanaga Island at Round Head, just north of Weed Bight (fig. 3). This cone is truncated by a seacliff that exposes a 50- to 70-m-thick sequence of olivine basalt lava flows. These rocks underlie and thus predate the volcanic rocks that make up Mount Kanaton.

Volcanic Rocks of Mount Kanaton

"Mount Kanaton" is the name that Coats (1956) used to describe a large ancestral shieldlike cone that surrounds the south flank of modern Kanaga Volcano (fig. 2). The volcanic rocks of ancestral Mount Kanaton include a 400- to 500-m-thick sequence of lava flows of basaltic andesite and andesite, volcanic breccia, and pyroclastic deposits that form most of Kanaton Ridge, a prominent scarplike feature sculpted into the side of Mount Kanaton (Coats, 1956). The lava flows exposed in the scarp of Kanaton Ridge dip gently (approx 15°) south, suggesting that the ancestral edifice was in about the same position as the modern cone of Kanaga Volcano. K-Ar ages of lavas from Kanaton Ridge indicate that Mount Kanaton was active in middle and late Quaternary time (Bradley Singer, unpub. data, 2001). Scattered deposits of till, striated and ice-molded bedrock, and U-shaped glacial valleys indicate that the south slopes of Mount Kanaton were formerly overrun by glacier ice. This area is mantled by peat and tephra deposits that began accumulating about 11 ka, suggesting that the edifice of Mount Kanaton was high enough to support glacier ice possibly associated with the latest worldwide glaciation, which peaked about 18 ka (Imbrie and others, 1983). Thus, the bulk of ancestral Mount Kanaton could have been constructed by at least Pleistocene time.

Modern Cone of Kanaga Volcano

The modern cone of Kanaga Volcano is a composite stratocone composed of interbedded andesitic lava flows and pyroclastic debris. Typical lava flows on the cone have blocky aa surface morphology, well-defined marginal levees, and distinct lobate flow fronts (figs. 2, 3). All of the major flows appear to have been erupted from the central vent and several fresh-appearing, unvegetated lava flows and flow fields (Ql_{94}, Ql_{06}, Qlh, fig. 3) are identifiable on the east-northeast, south, southwest, west-southwest, and northwest flanks of the volcano. Lava flows on the southwest, west-southwest, north, and northwest flanks of the volcano extend to the ocean. Older lava flows and flow fields (Qlcb, fig. 3) are vegetated to varying degrees and locally mantled with tephra but still retain fresh-appearing surface features. Most of the lava flows that make up the edifice of Kanaga Volcano are medium-K and calc-alkaline in composition (fig. 4) and composed primarily of porphyritic two-pyroxene andesite and basaltic andesite;

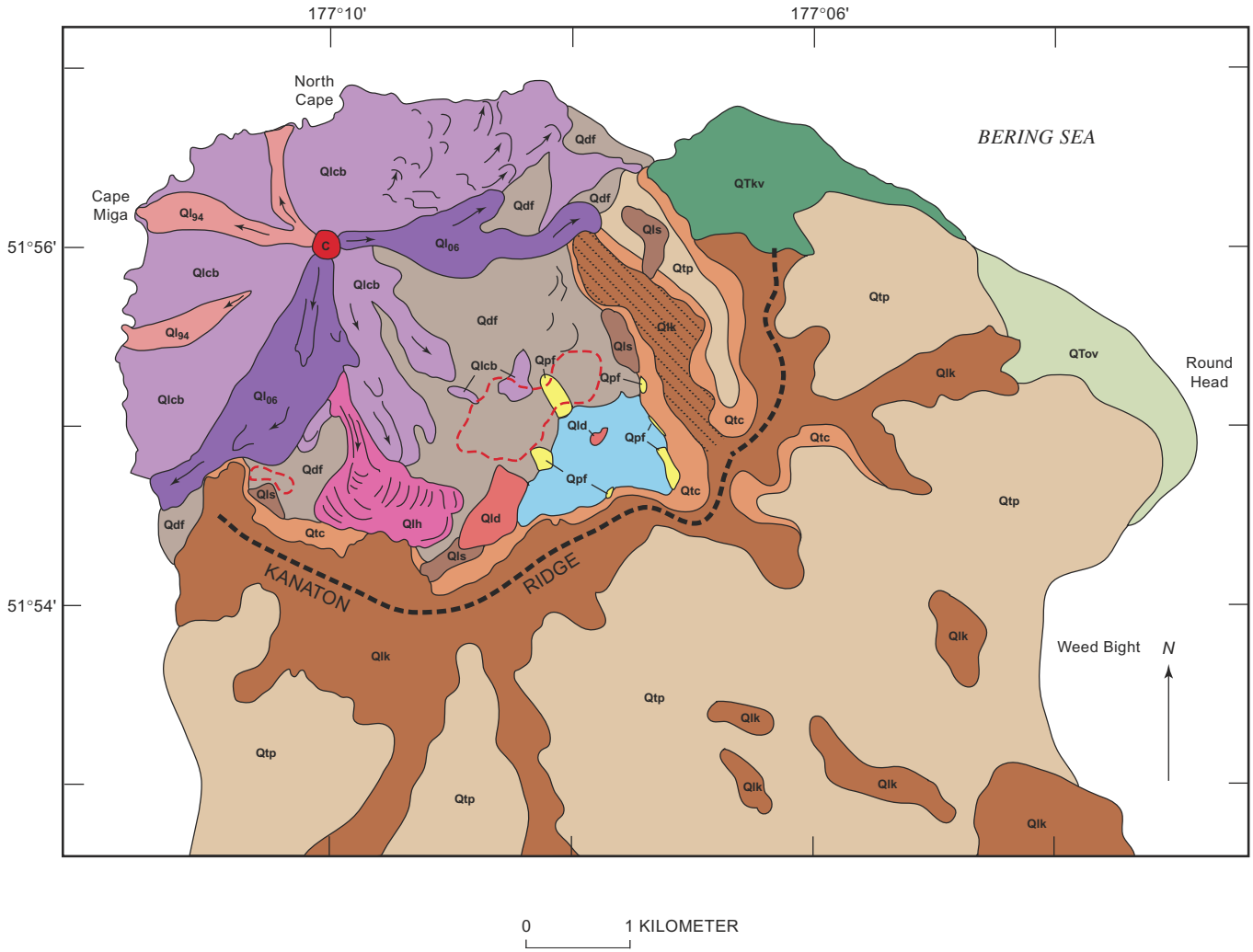

EXPLANATION

Lava flows of historical eruptions

- Ql_{94} — Andesite flows erupted in 1994.
- Ql_{06} — Andesite flows erupted in 1906.

Qlh — **Lava flow (Holocene)**—Andesite aa lava flow produced by historical(?) eruption of Kanaga Volcano

Qlcb — **Lava flows (Holocene)**—Lava flows produced by prehistorical and older eruptions of Kanaga Volcano; may include areas of blocky talus and avalanche debris

Qpf — **Pyroclastic-flow deposits (Holocene)**—Pumiceous pyroclastic-flow deposits associated with eruptions from vents on the southeast flank of Kanaga Volcano

Qdf — **Lahar and lahar run-out deposits (Holocene)**—Poorly sorted, fan-shaped deposits of boulders, gravel, sand, and silt deposited by water-saturated mixtures of volcaniclastic debris during eruptions; may contain juvenile clasts of dacite and andesite

Qtp — **Tephra, soil, and peat deposits (Holocene)**—Blanketing mantle of airfall tephra, buried soils, and peat, 1-3 m thick; may include colluvial deposits

Qls — **Landslide deposits (age uncertain)**—Intact to partially dissaggregated blocks of andesitic lava derived from the rim of Kanaton Caldera

Qtc — **Talus and other colluvial deposits (Holocene)**—Rock rubble, solifluction deposits, and rockfall debris on slopes

Qld — **Lava domes (Holocene?)**—Andesitic lava domes on the southeast flank of Kanaga Volcano

Qlk — **Lava flows erupted from Mount Kanaton (Pleistocene and Pliocene?)**—Andesitic cone-building lava flows of ancient Kanaton Volcano. Ruled pattern indicates slump block associated with caldera collapse

QTkv — **Lava flows older than Kanaton volcano (Quaternary or Tertiary)**—Basaltic lava flows erupted from vents on or near the north coast of Kanaga Island

QTov — **Lava flows erupted from vents offshore of Kanaga Island (Quaternary or Tertiary)**—Basaltic lava flows and breccia associated with no-longer-active vents offshore of Kanaga Island

C — **Crater of Kanaga Volcano**

Flow margins of lava flows

Flow path of lava flows

Collapse-caldera margin

Field of ballistic-impact craters

Figure 3. Generalized geologic map of Kanaga Volcano (fig. 1).

phenocrysts are chiefly plagioclase, clinopyroxene, orthopyroxene, and Fe oxide minerals, with traces of olivine and hornblende. The groundmass is typically a pale- to light-brown glass containing microlites of plagioclase and pyroxene. Systematic variations in mineralogy or whole-rock chemistry are not apparent, suggesting that the composition of the Kanaga lava flows has changed little over time.

Pumice-Bearing Deposits

Pumice-bearing pyroclastic-fall, pyroclastic-flow, and lahar deposits are preserved on the south flanks of Kanaga Volcano (fig. 3), and pumice lapilli tephra deposits are common on the south slopes of Kanaton Ridge. The pyroclastic-flow and lahar deposits, which are fresh, unvegetated, and little modified, are the eruptive products of relatively recent explosive eruptions. Pumice from the pyroclastic-flow, lahar, and tephra deposits is more silicic (63–66 weight percent SiO_2) than the predominant andesite of Kanaga Volcano (fig. 4), and eruptions involving dome collapse are the most likely origin for these deposits; however, lava domes of dacitic composition have not been identified at Kanaga Volcano. The position and pumice clast size (granule to cobble) of the pyroclastic deposits suggests that their parent domes may have been buried by younger lava flows erupted from the summit vent.

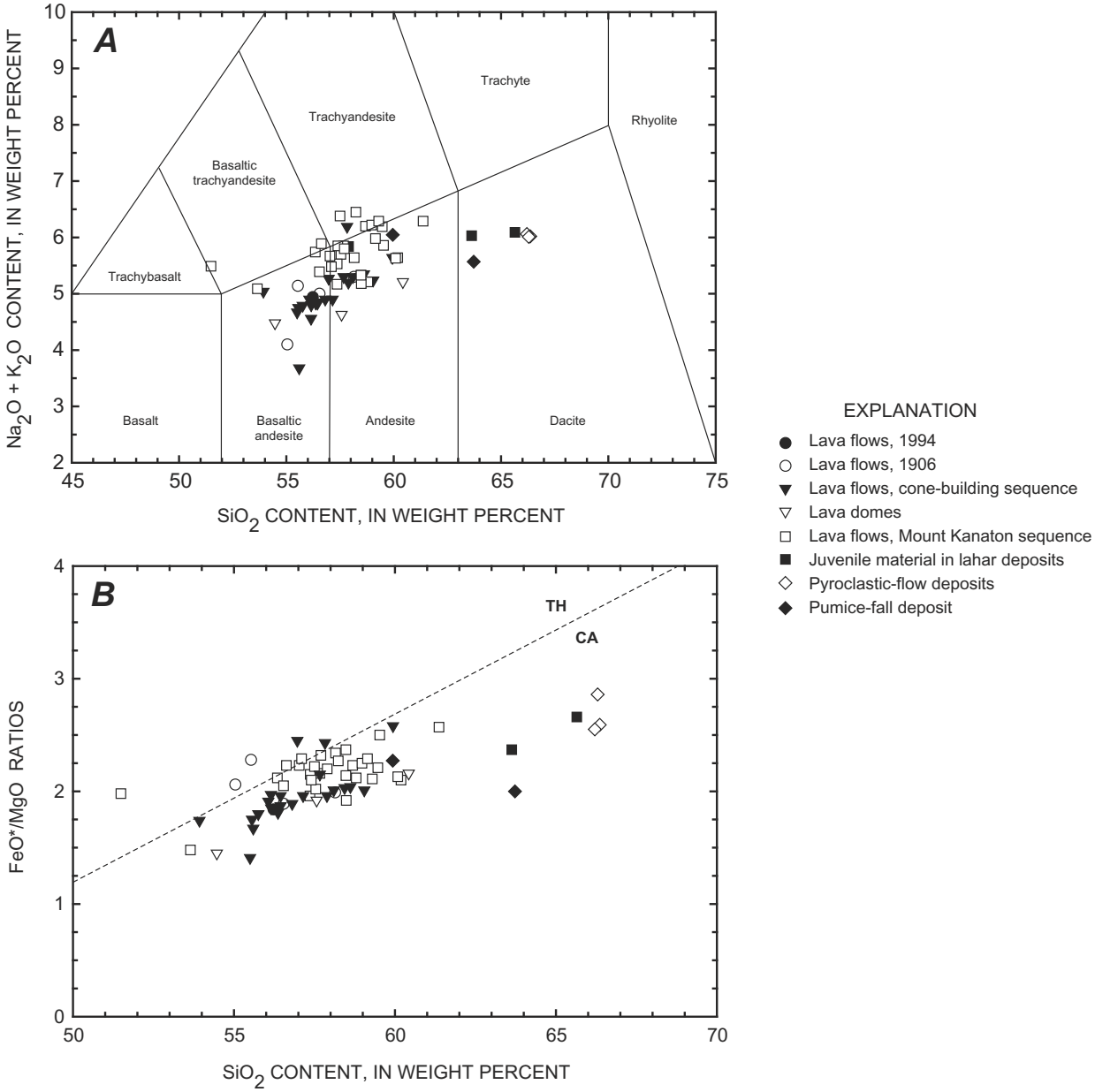

Figure 4. Compositional plots for lava flows and pyroclastic deposits from northern Kanaga Island (fig. 1). *A*, Na_2O+K_2O versus SiO_2 contents. Discriminant lines from Le Bas and others (1986). *B*, FeO^*/MgO ratio versus SiO_2 content. plot for lava flows and pyroclastic deposits from northern part of Kanaga Island. Tholeiite/calk-alkaline discriminant line from Miyashiro (1974).

Lava Domes

Andesitic lava domes are exposed in the southern part of the caldera in and adjacent to the intracaldera lake (fig. 5). These domes, which are compositionally different from the silicic pumice in tephra deposits on the flanks of the volcano (fig. 4), are believed to have been emplaced during an earlier eruptive phase more closely related to the modern andesite edifice. The age of the domes is not known, but they appear little weathered and are overlain by pyroclastic-flow deposits erupted 1.3–0.9 ka.

Eruptive History

Edifice Collapse

The modern cone of Kanaga Volcano is partly surrounded by Kanaton Ridge, a prominent semicircular scarp cut into the side of ancestral Mount Kanaton (fig. 3). The scarp is either the remnant of a typical island-arc collapse caldera now breached to the northwest, or the scarp of an avalanche caldera resulting from a northwestward-directed edifice failure. Our reconstruction of ancestral Mount Kanaton indicates a volcano with a basal diameter of about 13 km, an estimated elevation of about 2.3 km above sea level, and a volume of at least 75 km^3. We estimate that at least a third (approx 25 km^3) of Mount Kanaton has been removed by structural collapse. Typical collapse calderas in the Aleutian Arc are surrounded by voluminous pyroclastic-flow and tephra deposits emplaced during catastrophic caldera-forming eruptions (Miller and Smith, 1987). Such deposits form sheetlike accumulations of pumiceous pyroclastic debris that are tens of meters thick and extend radially from the caldera for many tens of kilometers. The geologic map of the northern part of Kanaga Island by Coats (1956) shows an extensive area of andesite tuff south and east of Kanaga Volcano. Before our work, we assumed that the andesite tuff mapped by Coats (1956) was likely the pyroclastic flow sheet generated by the caldera-forming eruption which formed Kanaton Ridge. To the contrary, we discovered that pyroclastic-flow deposits are rare on Kanaga Island and that the andesite tuff of Coats (1956) consists mostly of interbedded peat and felsic tephra deposits. These tephra deposits, though abundant, are insufficiently thick or coarse to represent a caldera-forming eruption and are absent in some areas where deposition would be expected. Deposits of pumice-rich, crossbedded alluvium that were discovered in the central part of Kanaga Island indicate that periods of explosive silicic volcanism have occurred in the past. Pumice in these deposits is reworked and may have been generated by explosive eruptions of Mount Kanaton, but we are uncertain whether the pumice was initially emplaced during a caldera-forming eruption.

These observations may be explainable if the formation of Kanaton Ridge occurred in Pleistocene time. Glaciation of the northern part of Kanaga Island could have removed some of the deposits generated by a caldera-forming eruption; however, it is unlikely that all such deposits would have been removed by glaciers and deposits of till which we did observe to contain no pumiceous material. The absence of voluminous pyroclastic-flow deposits on the flanking slopes of Mount Kanaton does not necessarily mean that a caldera-forming eruption did not occur, because elsewhere in the Aleutian Arc where Pleistocene calderas have been identified (for example, Emmons Lake and Ugashik Caldera on the Alaska Peninsula), pyroclastic-flow deposits are somewhat sparse and have limited aerial distribution. However, radiocarbon dating of buried soils and peat associated with conspicuous tephra deposits on Kanaga Island yields no evidence of major caldera-forming eruptions of Holocene age. Thus, if Kanaton Ridge is the scarp of a collapse caldera, it must have formed before the Holocene. Kanaton Ridge could be

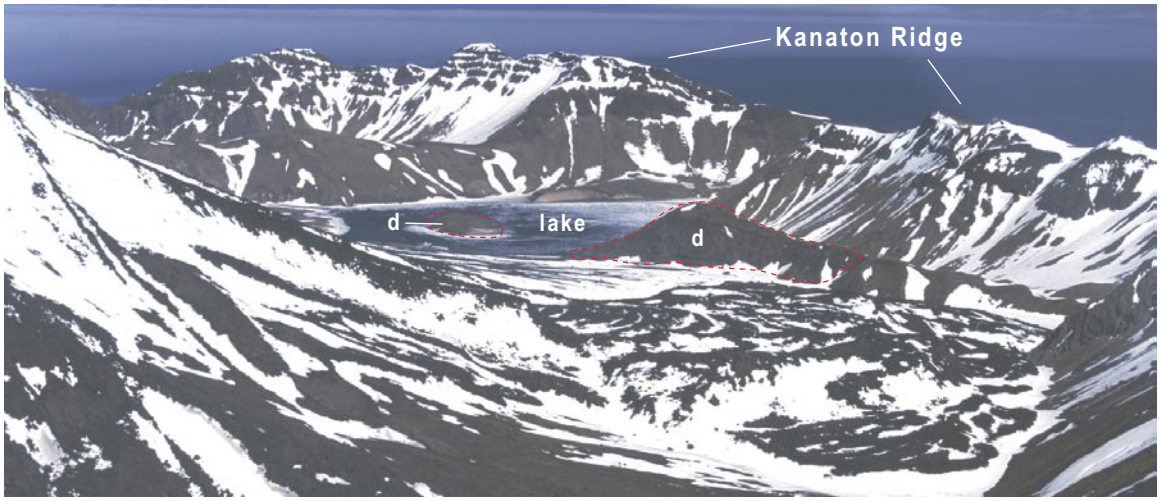

Figure 5. South flank of Kanaga Volcano, showing intracaldera lake (fig. 1), and Kanaton Ridge. Area d (outlined with red dashed line), lava domes of andesitic composition. These domes are not dated but are overlain by pyroclastic-flow deposits erupted about 1,000 yr B.P. View southeastward; photograph by C.F. Waythomas, taken July 2000.

a somma-like feature representing the headscarp of a northward-directed edifice failure. This failure may not have been associated with a major eruption and thus could have occurred without leaving extensive pyroclastic-flow deposits on Kanaga Island.

Images of the sea floor in the southern Bering Sea near Kanaga Island made during the GLORIA project (EEZ-Scan scientific staff, 1991) show an area of irregular, hummocky topography extending northwestward from Kanaga Island (fig. 6). This feature could be a debris-avalanche deposit that formed when the northwest sector of ancestral Mount Kanaton foundered into the sea. The length (L) of the feature is 38 km, measured from the presumed headscarp at Kanaton Ridge to its terminus, and the average width is 12 km, giving an area of about 460 km^2. We estimated the height (H) of ancestral Mount Kanaton at about 2,300 m, giving an H/L ratio of 0.06, a low value consistent with the long runout expected for submarine landslides (Holcomb and Searle, 1991). The width of the initial slide block is about 10 km, as estimated from the scarp width, and the minimum height of the scarp, as determined from a topographic profile (fig. 7), is about 500 m.

The tectonic architecture of the western Aleutian Arc is characterized by a series of rhomb-shaped crustal blocks of various sizes, from tens to hundreds of kilometers long (Geist and others, 1988). Subduction along the Aleutian Trench during late Cenozoic time has caused clockwise rotation of these blocks. Block rotation leads to the formation of many throughgoing strike-slip faults within the rotated massifs. However, late Cenozoic volcanic centers apparently occur in areas of unrotated crust and are beyond the limit of deformation associated with block rotation (Geist and others, 1988), suggesting that structural controls on volcanic-edifice stability may be less important than if the volcanoes were situated on structurally complex blocks of rotated crust. We did not observe any major faults on or near ancestral Mount Kanaton, nor did Coats (1956), who mapped several small faults around Kanaton Ridge. Reactivation of structures in the subvolcanic basement has been proposed as a mechanism for volcanic-edifice collapse (van Wyk de Vries and Francis, 1997; Vidal and Merle, 2000), but given the tectonic setting of Kanaga Volcano described above, this mechanism seems unlikely to have caused the collapse of ancestral Mount Kanaton.

Oceanic volcanoes, especially those in active volcanic arcs, commonly show evidence of former flank failures (Holcomb and Searle, 1991). Collapse processes are complex and commonly interrelated but almost always involve some type of magmatic activity (McGuire, 1996; Voight and Elsworth, 1997; Keating and McGuire, 2000). During our studies of Kanaga Volcano, we discovered several lava domes near the base of the scarp that defines Kanaton Ridge (fig. 3). Although the dome rocks have not been dated, they are chemically distinct from tephra deposits of Holocene age on the island and may have been emplaced during a period of magmatic activity that predates the formation of the modern volcanic edifice. The oldest dated tephra was erupted about 11 ka, suggesting that the domes may be pre-Holocene. Although it is difficult to determine the mechanism(s) that initiated failure of ancestral Mount Kanaton, the presence of a lava-dome complex at the base of Kanaton Ridge may be more than coincidental. Intrusion of the dome complex could have destabilized the north flank of Mount Kanaton through a combination of mechanical, thermal, and, possibly, seismic processes associated with the ascending magma. Hydrous magma that intrudes colder host rocks and begins to cool and crystallize will release volatile materials. At shallow depths, the volume increase associated with magma degassing can be significant and may generate substantial water pressures (Burnham, 1979; Voight and Elsworth, 1997). Such pressures can theoretically exceed 100

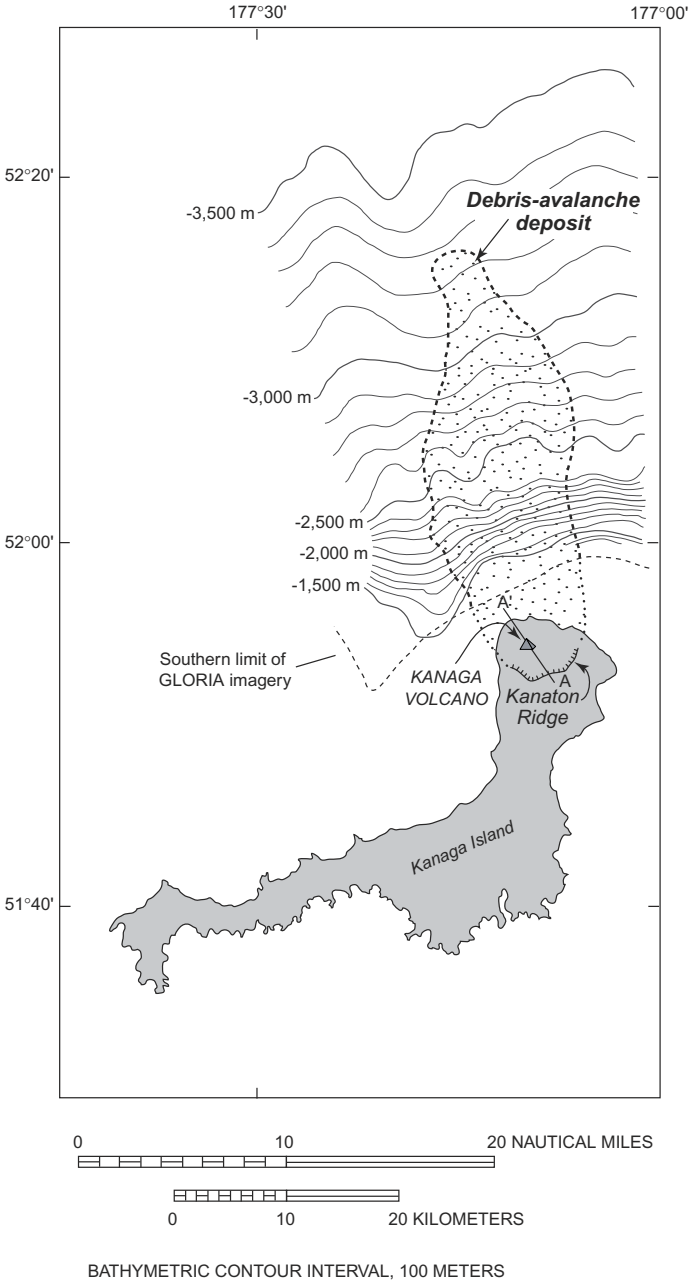

Figure 6. Bathymetry and approximate extent of debris-avalanche deposit north of Kanaga Island (fig. 1). Bathymetric data from Bering Sea (EEZ-Scan scientific staff, 1991).

MPa, whereas typical wallrock strength is less than about 20 MPa (Voight and Elsworth, 1997). Thus, a magmatic intrusion can initiate fractures that may become potential failure surfaces. A likely area for the formation of such fractures and potential planes of failure is the zone above the intrusion. Another effect of the intruding magma is to elevate pore pressures along the potential failure surface. A theoretical analysis of this effect (Elsworth and Voight, 1995; Voight and Elsworth, 1997; Voight, 2000) indicates that thermally induced pore-pressure changes could be sufficient to destabilize an oceanic volcano flank with the dimensions and geometry we estimate for ancestral Mount Kanaton. This scenario would require some rather extreme conditions, and the thermal forcing and diffusivity parameters associated with thermally driven ground-water flow would have to be maximums (Voight and Elsworth, 1997). However, the combined effects of mechanical, thermal, and seismically induced changes in pore pressure associated with magma emplacement could be sufficient to destabilize the edifice and initiate failure, as they have for other volcanoes, such as Mount St. Helens (Voight and others, 1983). In the absence of strong evidence for a collapse caldera, we suggest that Kanaton Ridge is the headscarp of an avalanche caldera which formed when the north flank of ancestral Mount Kanaton was displaced seaward by a shallow magmatic intrusion.

Tephrostratigraphy

Tephra deposits of Holocene age are common on Kanaga Island, and most of the area south of Kanaton Ridge (fig. 3) is covered by several meters of interbedded tephra, peat, and soil (fig. 8). Samples of the soil organic matter associated with many of the more conspicuous tephra beds were collected from various stratigraphic profiles around the island (fig. 9) and dated by conventional radiocarbon techniques (table 1).

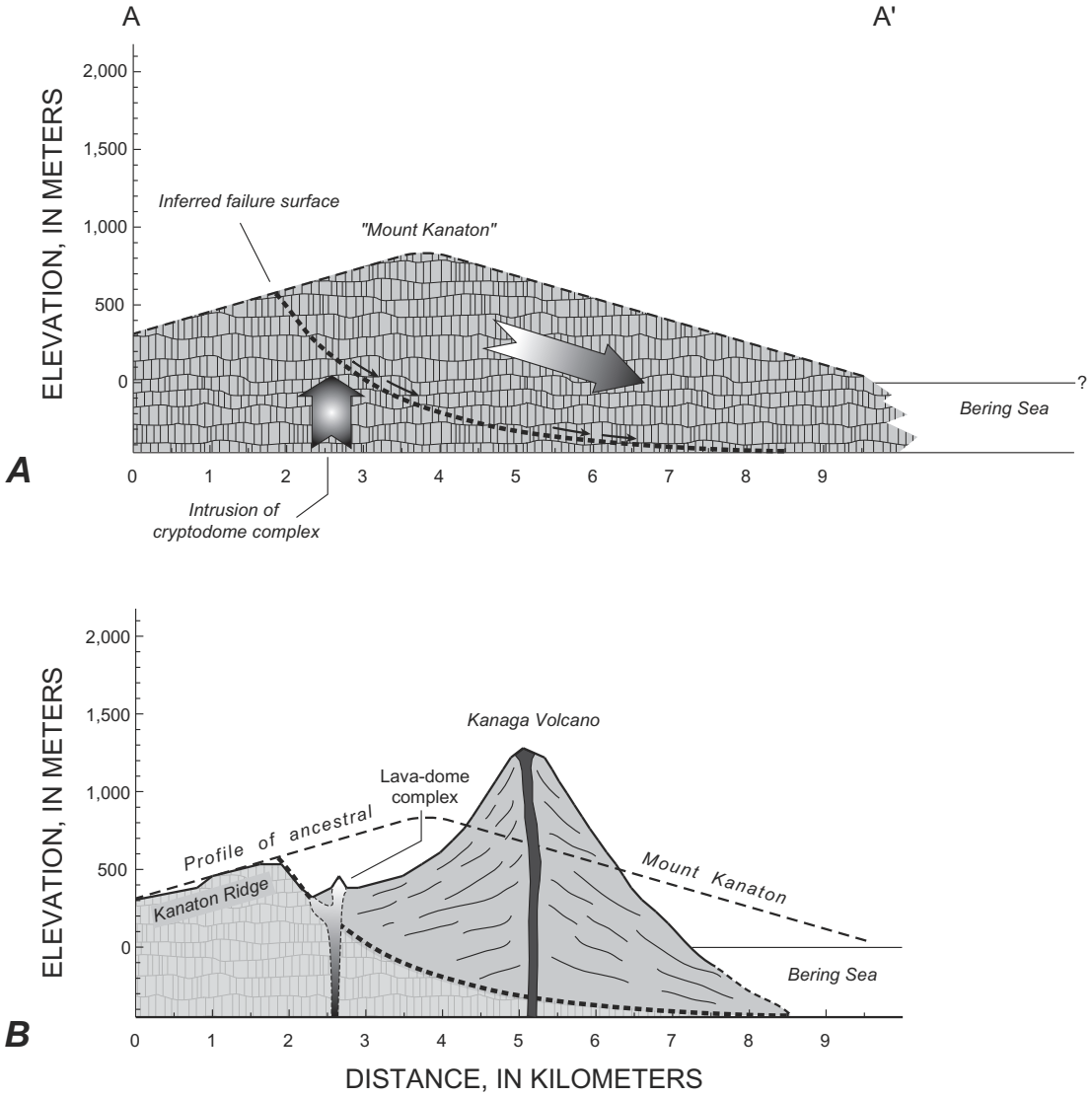

Figure 7. Simplified geologic cross sections of Mount Kanaton and Kanaga Volcano (fig. 1). *A*, Ancestral Mount Kanaton, showing inferred failure surface and location of cryptodome complex. *B*, Modern Kanaga Volcano. Line of cross section *A*–*A'* for both cross sections is shown in figure 6.

Table 1. Radiocarbon ages on samples from Kanaga Island.

[All ages in ^{14}C years before present (=A.D. 1950). Radiocarbon ages obtained from humic acid fraction of soil organic matter (except for sample 98CW68–7, which was obtained from peat), calibrated by the method of Stuiver and Reimer (1993). Calibrated ages listed in bold, flanked by 2σ error-limit ages]

Sample	Laboratory No.	Location (lat N., long W.)	Reported age (yr B.P.)	$\delta^{13}C$ value (permil)	Calibrated age (yr B.P.)
99CW68–7	GX–26011–LS	51°53′, 177°05′	Modern (102.98±0.73% present ^{14}C activity)	–27.3	– – –
99CW68–6	GX–26010–LS	51°53′, 177°05′	475±60	–26.2	623, 514, 337
00CW21–2	GX–27881	51°53′, 177°07′	500±60	–28.8	640, 524, 467
99CW76–2	GX–26021	51°52′, 177°03′	590±80	–27.0	672, 621, 607, 555, 505
00CW21–4	GX–27889	51°53′, 177°07′	890±60	–30.7	931, 789, 674
00CW08–2	GX–27886	51°53′, 177°07′	1,180±100	–28.1	1,293, 1,065, 925
99CW68–2	GX–26008	51°53′, 177°07′	1,390±110	–25.8	1,523, 1,294, 1,062
00CW21–6	GX–27882	51°53′, 177°07′	1,800±60	–27.6	1,873, 1,721, 1,559
00CW14–1	GX–27884	51°54′, 177°07′	1,850±120	–27.6	2,045, 1,817, 1,522
00CW21–8	GX–27888	51°53′, 177°07′	2,680±90	–28.4	2,956, 2,775, 2,512
99CW75–1	GX–26018	51°52′, 177°11′	3,100±90	–27.0	3,474, 3,342, 3,276, 3,273, 3,076
99CW83–5	GX–26029–LS	51°41′, 177°17′	3,310±60	–28.2	3,690, 3,551, 3,508, 3,483, 3,390
99CW75–3	GX–26019	51°52′, 177°11′	3,420±170	–24.6	4,146, 3,686, 3,660, 3,642, 3,271
99CW68–4	GX–26009–LS	51°53′, 177°05′	3,490±110	–26.1	4,085, 3,813, 3,792, 3,757, 3,751, 3,723, 3,472
99CW54–4	GX–25997	51°49′, 177°09′	3,630±140	–25.6	4,408, 3,961, 3,949, 3,927, 3,578
99CW82–1	GX–26027–LS	51°41′, 177°17′	3,720±70	–25.4	4,725, 4,086, 4,025, 4,020, 3,868
99CW77–4	GX–26022–LS	51°52′, 177°05′	3,790±70	–25.1	4,413, 4,151, 3,931
99CW83–4	GX–26028–LS	51°41′, 177°17′	3,850±60	–29.0	4,420, 4,244, 4,088
00CW22–5	GX–27890	51°51′, 177°07′	3,940±140	–26.5	4,829, 4,413, 3,934
00CW23–4	GX–27891	51°52′, 177°07′	3,910±200	–27.3	4,856, 4,406, 4,365, 4,363, 3,731
00CW06–4	GX–27879	51°57′, 177°06′	4,940±150	–26.7	5,989, 5,655, 5,322
99CW77–5	GX–26023–LS	51°52′, 177°05′	5,760±70	–25.9	6,728, 6,548, 6,406
99CW54–3	GX–25996	51°49′, 177°09′	5,740±170	–25.4	6,910, 6,499, 6,200
99CW75–7	GX–26020	51°52′, 177°11′	6,120±110	–25.3	7,267, 6,990, 6,684
99CW55–2	GX–25998–LS	51°48′, 177°12′	6,740±90	–25.1	7,745, 7,606, 7,602, 7,587, 7,432
00CW23–1	GX–27878	51°52′, 177°07′	8,310±210	–26.1	9,700, 9,398, 9,372, 9,358, 9,349, 9,342, 9,300, 8,641
99CW52–1	GX–25995	51°50′, 177°08′	8,470±330	–25.4	10,240, 9,490, 8,592
99CW77–10	GX–26025	51°52′, 177°05′	9,140±130	–26.0	10,668, 10,240, 9,919
00CW22–1	GX–27880	51°51′, 177°07′	9,270±500	–26.8	12,104, 10,482, 10,442, 10,428, 9,163
99CW77–9	GX–26024	51°52′, 177°05′	9,760±140	–25.6	11,553, 11,181, 10,694

Figure 8. Typical exposure of pyroclastic-fall deposits and buried soils on Kanaga Island (fig. 1). Most light-colored beds are tephra deposits from Kanaga Volcano; dark layers are buried A soil horizons.

Radiocarbon dating of A soil horizons immediately below a tephra bed yields information about the timing of tephra deposition and allows us to outline a preliminary chronology of Holocene tephra-producing eruptions for Kanaga Volcano. Although we have not yet completed our analysis of the glass chemistry of the tephra deposits as a correlation aid, we can correlate various tephra deposits on the basis of their associated radiocarbon ages and field characteristics (fig. 11). Groups of tephra deposits so defined indicate that at least 11 eruptions of Kanaga Volcano have occurred since about 11 ka. Most of these eruptions were probably sub-Plinian to Plinian, producing moderately vesicular dacitic pumice lapilli tephra deposits ranging in thickness from a few centimeters to more than 1 m (table 2).

Studies of tephra deposits on nearby Adak Island (fig. 9) have yielded information on the age and chemistry of most of the major tephra deposits (fig. 12), many of which are believed to have been erupted from Kanaga Volcano (Black, 1980; Romick and others 1992; Kirianov and Miller, 1997). Correlation of the tephra records from Adak and Kanaga Islands based on the radiocarbon ages of the major tephra deposits indicates that only two of the major Adak tephras (the basal pink ash of Kiriyanov and Miller, 1997, and the Yellow-Brown-Olive Ash of Black, 1980) have age-equivalent tephra deposits on Kanaga Island (fig. 13). These results imply that the three thickest tephra deposits on Adak Island—the Main, Intermediate, and Sandwich Ashes of Black (1980)—are not readily identifiable as eruptive products from Kanaga Volcano and could record substantial Holocene eruptions from other volcanoes, including Mount Moffett on the northern part of Adak Island. The most conspicuous tephra deposit on Adak Island, the Main Ash, has long been regarded as the pyroclastic-fall deposit associated with the caldera-forming eruption that destroyed ancestral Mount Kanaton (Coats, 1956; Black, 1980). However, none of the dated tephra deposits on Kanaga Island matches the radiocarbon ages associated with the Main Ash (fig. 13). A thick lapilli tephra deposit about the same age as the Intermediate Ash is present at locality 00CW06 northeast of Kanaga Volcano (fig. 9) but is not recognized elsewhere on Kanaga Island. Radiocarbon ages associated with Kanaga Island tephra T7 match those of the Sandwich Ash (fig. 13); however, the T7 deposits consist of massive sand-size felsic tephra with granule-size juvenile lapilli at the base (sec. 99CW75, fig. 9) or a single thin lapilli bed (sec. 99CW83, fig. 9) and do not exhibit the sequence massive gray fine ash/

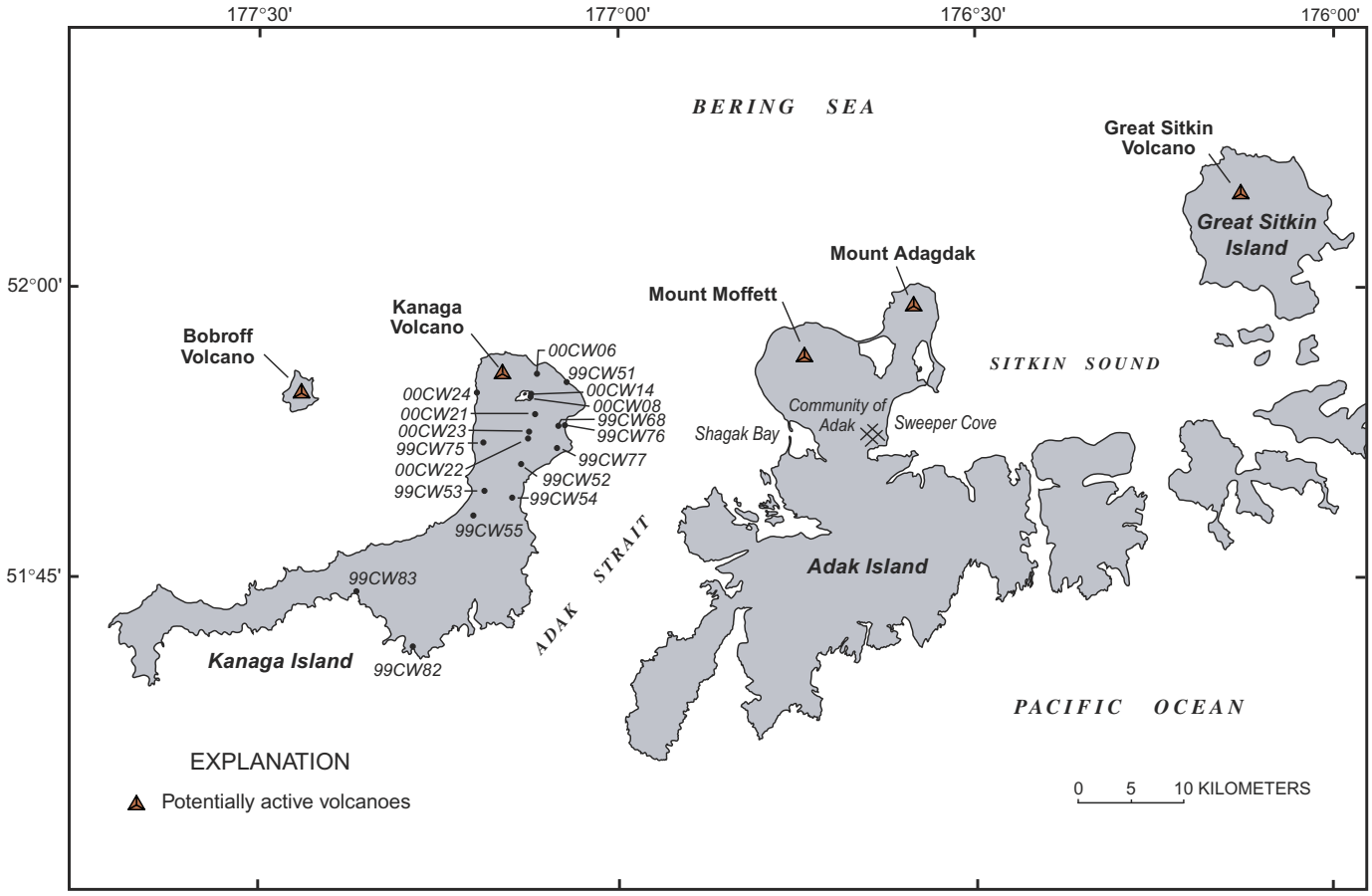

Figure 9. Western part of the Aleutian Islands, Alaska (fig. 1), showing locations of measured stratigraphic sections on Kanaga Island and other islands and of local volcanoes. Station numbers refer to stratigraphic profiles shown in figure 10.

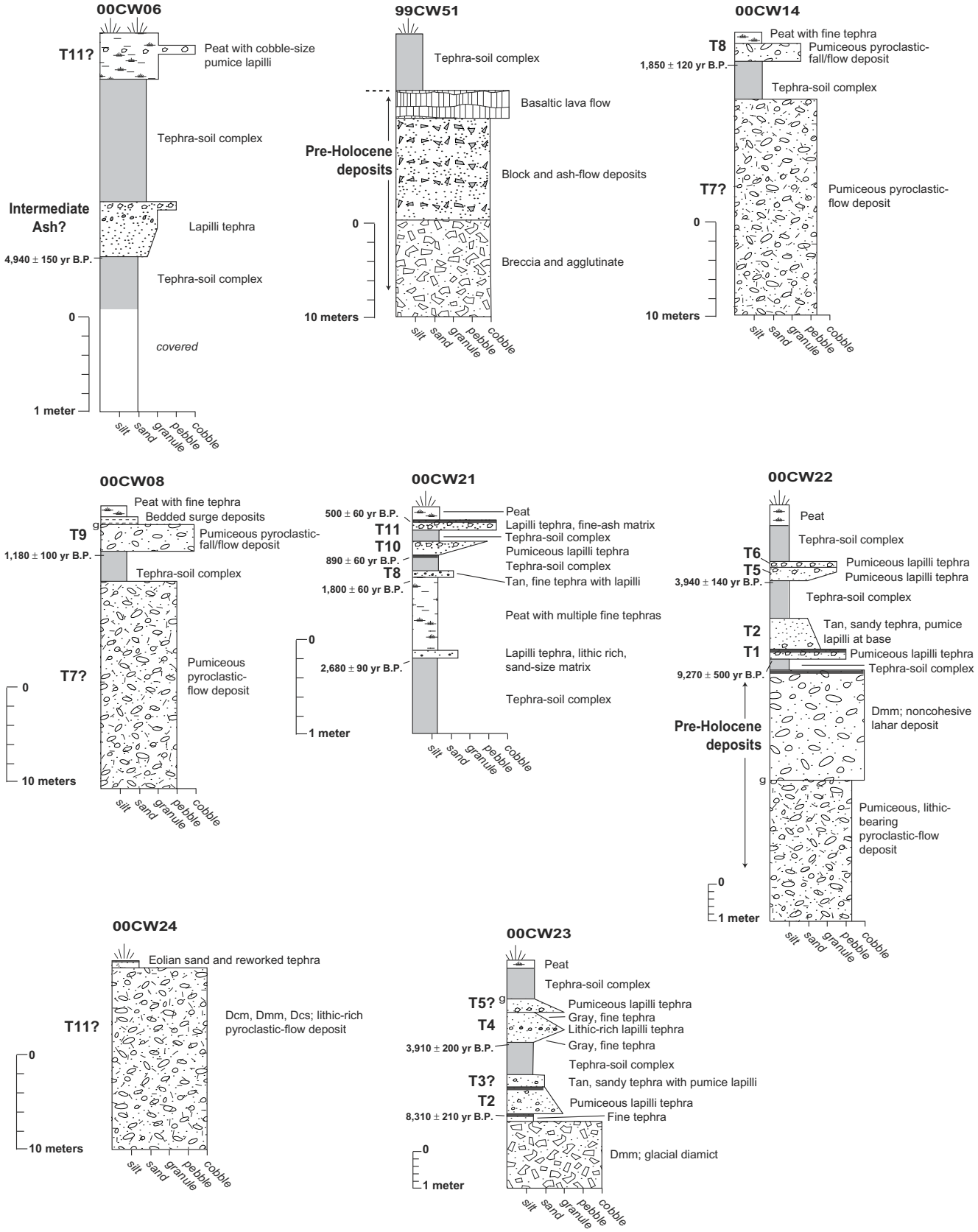

Figure 10. Stratigraphic profiles of surficial deposits on Kanaga Island (fig. 1), showing major tephra deposits, buried soils, and uncalibrated radiocarbon ages. Width of units is proportional to average particle size, as indicated by scale along base of each section. Locations of sections are shown in figure 9.

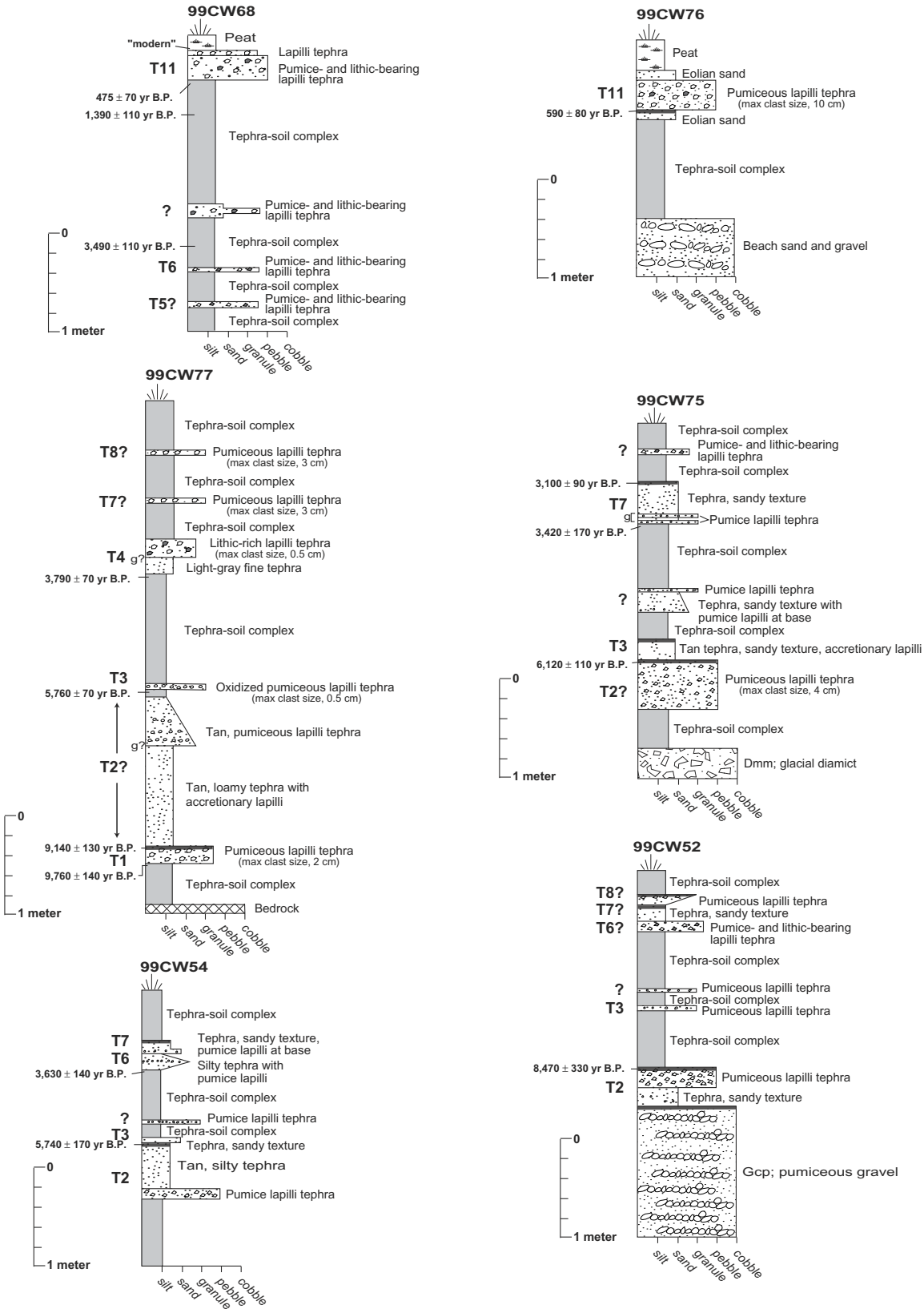

Figure 10.—Continued

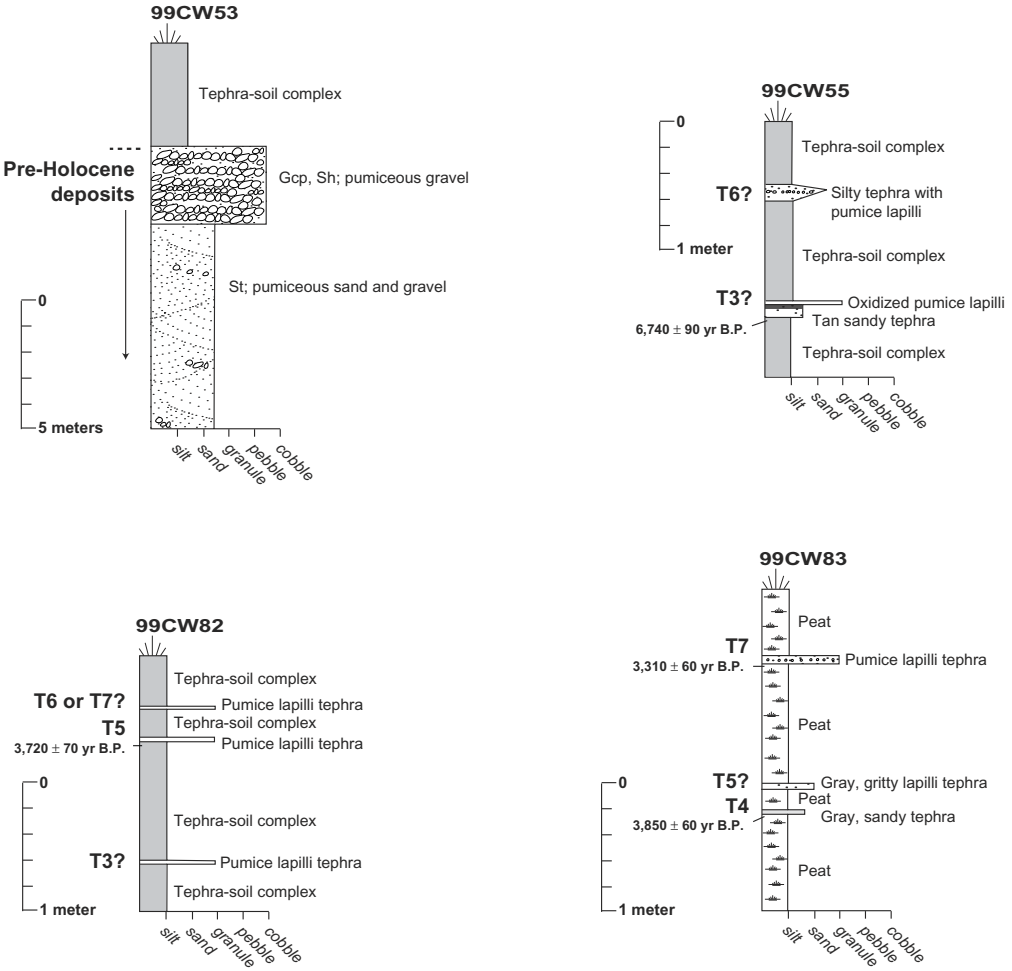

EXPLANATION

Pumice lapilli	
Lithic lapilli	
Tephra-soil complex. Multiple, fine thin tephras with A-Cox soils	
g	Gradational contact
A-Cox soil	
T	Tephra sample
C	Radiocarbon sample
R	Clast/rock sample
M	Matrix sample

Dcm	Diamict, clast-supported, massive
Dmm	Diamict, matrix-supported, massive
Dcs	Diamict, clast-supported, stratified
Gcp	Gravel, clast-supported, planar-bedded
Sh	Sand, horizontally bedded
St	Sand, trough-crossbedded

Figure 10.—Continued

Table 2. Characteristics of major tephra deposits erupted from Kanaga Volcano.

Tephra deposit	Thickness (cm)	Maximum particle size (mm)	Distance of known deposits from present vent (km)	Estimated age (yr B.P.)
T1	15–20	30	5–10	10,300–11,100
T2	10–150	40	5–10	8,800–9,700
T3	4–30	5	5–15	6,500–6,800
T4	30–90	5	5–>15	4,100–4,400
T5	2–10	5	5–>15	3,900–4,300
T6	5–10	4	5–15	3,600–4,100
T7	2–40	5	5–>15	3,400–3,600
T8	8–100	50	0–5	1,600–1,900
T9	150	100	0–5	900–1,300
T10	7	15	0–5	700–900
T11	10–30	100	0–10	500–600

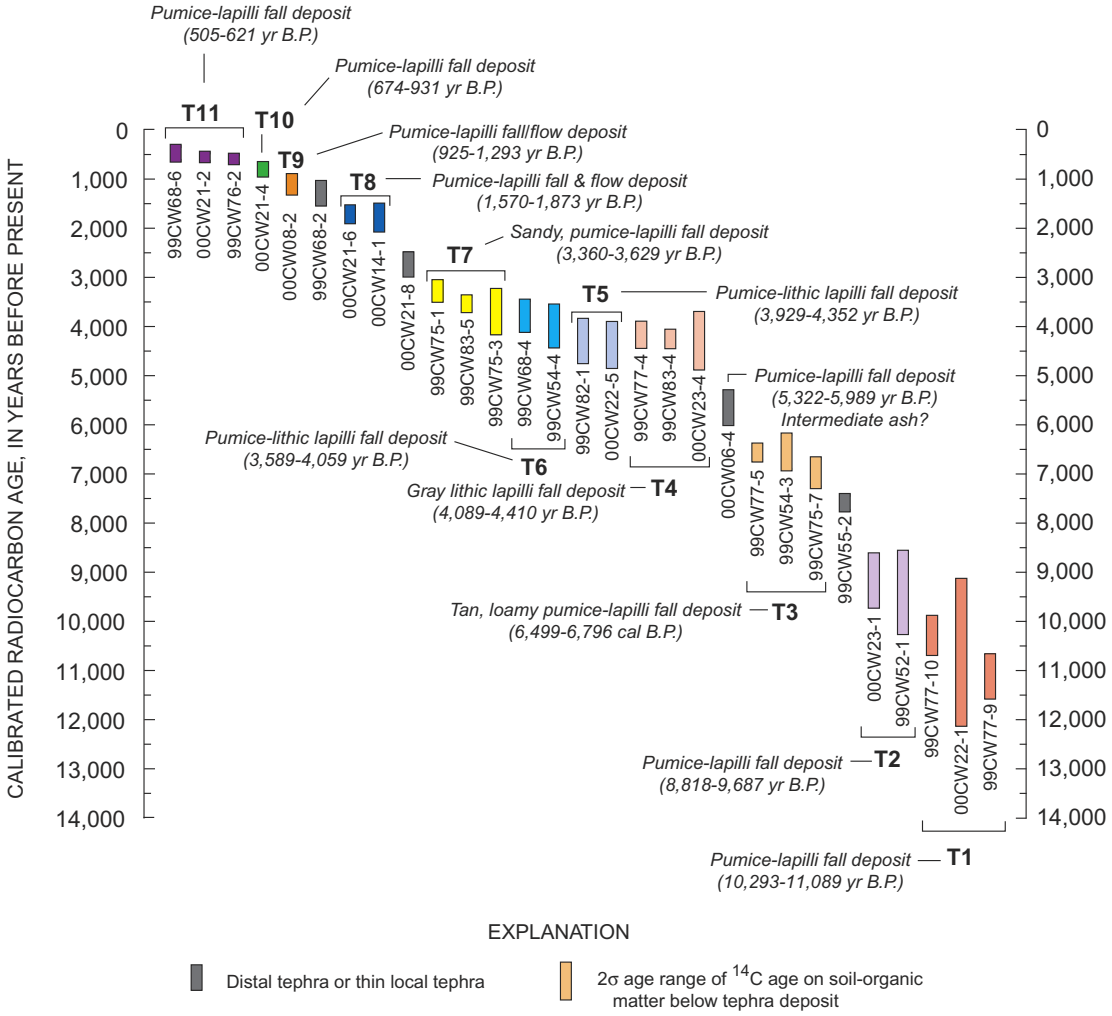

Figure 11. Correlation of tephra deposits on Kanaga Island (fig. 1), based on radiocarbon ages of buried soils. Vertical bars indicate 2σ age range for calibrated radiocarbon ages of buried soils associated with particular tephra deposit; numbers below bars denote radiocarbon samples listed in table 1. T1 through T11, preliminary groupings of tephra deposits based on radiocarbon ages and field characteristics of tephra deposits.

oxidized granule lapilli/massive gray fine ash that characterizes the Sandwich Ash on Adak Island. Thus, we are uncertain whether tephra T7 and the Sandwich ash are the same tephra deposit. The radiocarbon ages associated with tephra T8 on Kanaga Island and the Yellow-Brown-Olive Ash on Adak Island indicate that these two tephra deposits are temporally equivalent and are likely the same. The T8 deposits on Kanaga Island are coarser and thicker than deposits of the Yellow-Brown-Olive Ash on Adak, indicating that Kanaga Volcano was the likely source.

Conclusions

Our study of Kanaga Volcano reveals considerable new information about the history of the volcano as determined from stratigraphic studies of tephra deposits, radiocarbon dating of buried soils, and geologic mapping and chemical analysis of volcanic deposits. We have failed to locate credible evidence to support the hypothesis that Kanaton Ridge is the rim of a collapse caldera associated with a major pyroclastic eruption of Kanaga Volcano, as suggested by previous studies (Coats, 1956; Black, 1980). An area of hummocky topography observed in sea-floor imagery north of Kanaga Volcano appears to be a debris-avalanche deposit produced by a northward-directed edifice collapse of ancestral Mount Kanaton before the construction of the modern cone of Kanaga Volcano. Shallow magmatic intrusion of a cryptodome-like complex beneath ancestral Mount Kanaton is a plausible mechanism for destabilization of the edifice and subsequent flank collapse.

Our studies also indicate that Kanaga Volcano formed in the avalanche scar defined by Kanaton Ridge and was largely constructed in Holocene time. Tephra deposits erupted from Kanaga Volcano consist mainly of dense, moderately vesicular, coarse pumice lapilli of dacitic composition produced during explosive sub-Plinian to Plinian eruptions beginning about 11 ka. Correlation of tephra records on Kanaga and Adak Islands based on radiocarbon ages associated with major tephra beds indicates that few of the tephra deposits on Adak Island were produced by eruptions of Kanaga Volcano, as concluded by previous studies (Coats, 1956; Black, 1980; Romick and others, 1992; Kirianov and Miller, 1997). The source volcanoes for the three major middle Holocene tephra units on Adak Island (Main, Intermediate, and Sandwich Ashes) is uncertain, although Mount Moffett on the northern part of Adak Island now appears to be a likely source volcano.

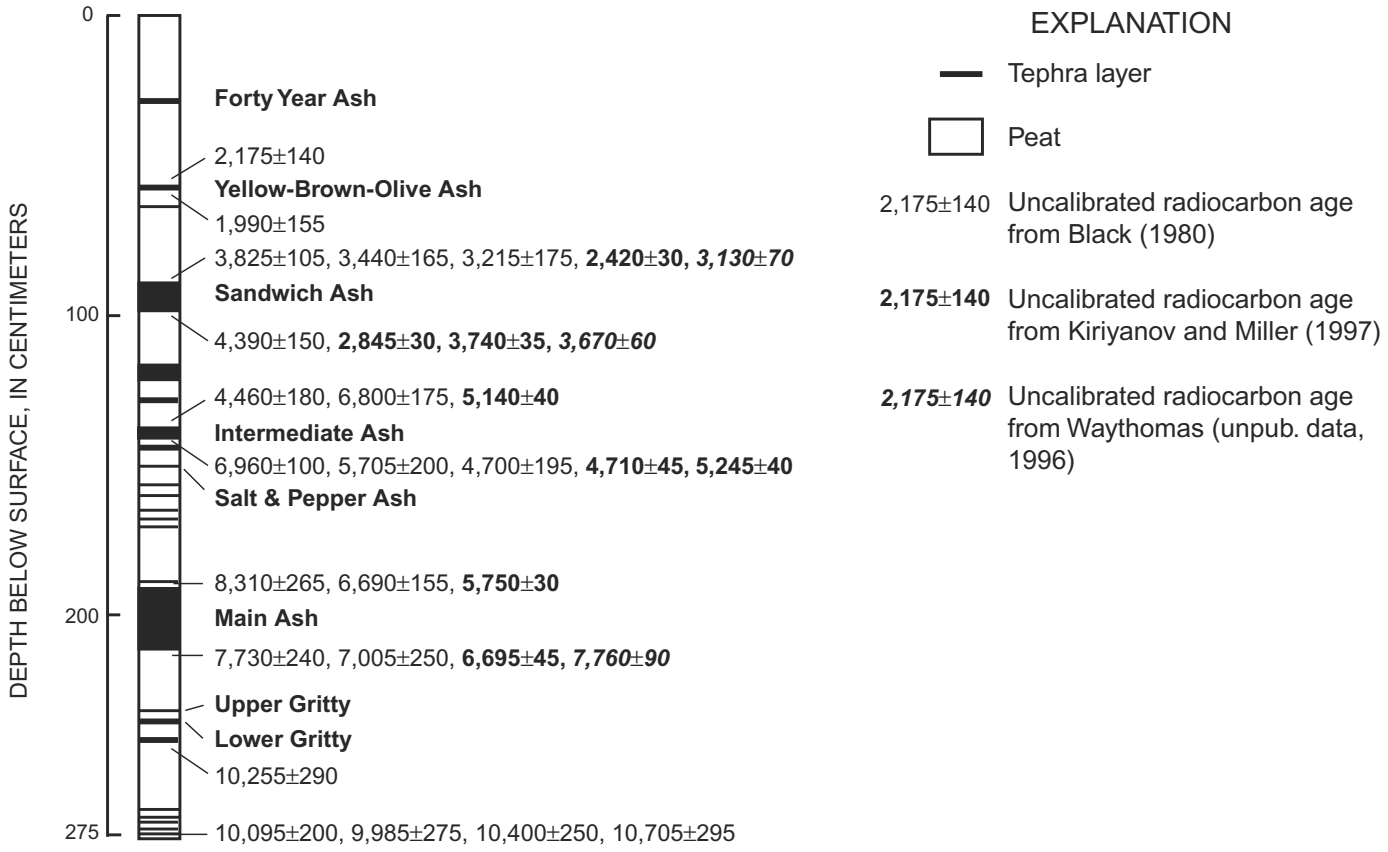

Figure 12. Tephrostratigraphic record from Adak Island (fig. 1). Modified from Black (1980).

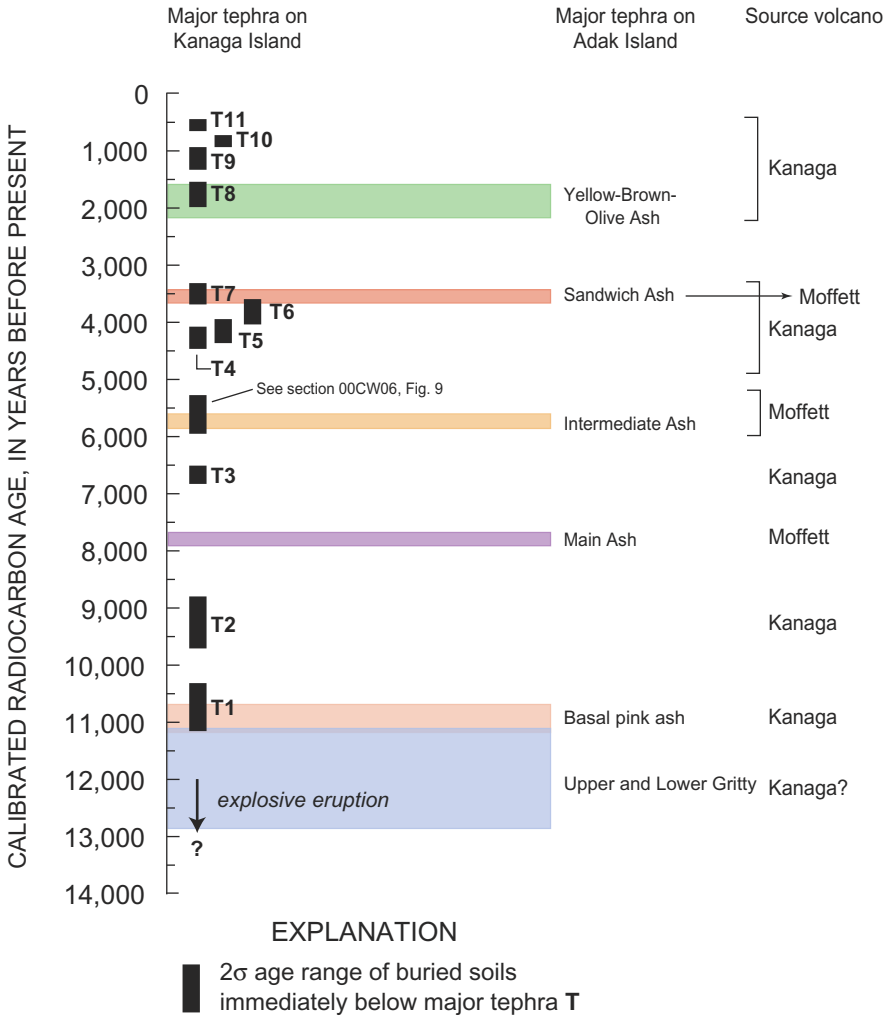

Figure 13. Correlation of tephra records from Kanaga and Adak Islands (fig. 1). Black vertical bars indicate calibrated 2σ age ranges of buried soils associated with major tephra deposits on Kanaga Island; colored bars indicate 2σ age ranges of buried soils associated with major tephra deposits on Adak Island.

References Cited

Black, R.F., 1980, Isostatic, tectonic, and eustatic movements of sea level in the Aleutian Islands, Alaska, *in* Morner, N.-A., ed., Earth rheology, isostasy, and eustasy: New York, John Wiley and Sons, p. 231–248.

Brophy, J.G., 1989, Can high-alumina arc basalt be derived from low-alumina arc basalt? Evidence from Kanaga Island, Aleutian Arc, Alaska: Geology, v. 17, no. 4, p. 333–336.

Brophy, J.G., 1990, Andesites from northeastern Kanaga Island, Aleutians—implications for calc-alkaline fractionation mechanisms and magma chamber development: Contributions to Mineralogy and Petrology, v. 104, no. 5, p. 568–581.

Burnham, C.W., 1979, Magmas and hydrothermal fluids, *in* Barnes, H.L., ed., Geochemistry of hydrothermal ore deposits (2d ed.): New York, John Wiley and Sons, p. 71–136.

Coats, R.R., 1956, Geology of northern Kanaga Island, Alaska: U.S. Geological Survey Bulletin 1028–D, p. 69–81.

EEZ-Scan scientific staff, 1991, Atlas of the U.S. Exclusive Economic Zone, Bering Sea: U.S. Geological Survey Miscellaneous Investigations Series Map I–2053.

Elsworth, Derek, and Voight, Barry, 1995, Dike intrusion as a trigger for large earthquakes and the failure of volcano flanks: Journal of Geophysical Research, v. 100, no. B4, p. 6005–6024.

Geist, E.L., Childs, J.R., and Scholl, D.W., 1988, The origin of summit basins of the Aleutian Ridge—implications for block rotation of an arc massif: Tectonics, v. 7, no. 2, p. 327–341.

Holcomb, R.T., and Searle, R.C., 1991, Large landslides from oceanic volcanoes: Marine Geotechnology, v. 10, no. 1–2, p. 19–32.

Imbrie, John, McIntyre, Andrew, and Moore, T.D., Jr., 1983, The ocean around North America at the last glacial maximum, *in* Porter, S.C., ed., The late Quaternary, v. 1 *of* Late Quaternary environments of the United States: Minneapolis, University of Minnesota Press, p. 230–236.

Keating, B.H., and McGuire, W.J., 2000, Island edifice failures and associated tsunami hazards: Pure and Applied Geophysics, v. 157, no. 6–8, p. 899–955.

Kiriyanov, V.Y., and Miller, T.P., 1997, Volcanic ashes of Adak Island, Aleutian Islands, Alaska: Volcanic Seismology, v. 19, no. 1, p. 65–78.

Le Bas, M.J., Le Maitre, R.W., Streckeisen, A.L., and Zanettin, B.A., 1986, Chemical classification of volcanic rocks based on the total alkali-silica diagram: Journal of Petrology, v. 27, no. 3, p. 745–750.

McGuire, W.J., 1996, Volcano instability—a review of contemporary themes, *in* McGuire, W.J., Jones, A.P., and Neuberg, Juergen, eds., Volcano instability on Earth and other planets: Geological Society of London Special Publication 10, p. 1–23.

Miller, T.P., and Smith, R.L., 1987, Late Quaternary caldera-forming eruptions in the eastern Aleutian arc, Alaska: Geology, v. 15, no. 5, p. 434–438.

Miller, T.P., McGimsey, R.G., Richter, D.H., Riehle, J.R., Nye, C.J., Yount, M.E., and Dumoulin, J.A., 1998, Catalog of the historically active volcanoes of Alaska: U.S. Geological Survey Open-File Report 98–582, 104 p.

Miyashiro, Akiho, 1974, Volcanic rock series in island arcs and active continental margins: American Journal of Science, v. 274, no. 4, p. 321–355.

Romick, J.D., Kay, S.M., and Kay, R.W., 1992, The influence of amphibole fractionation on the evolution of calc-alkaline andesite and dacite tephra from the central Aleutians, Alaska: Contributions to Mineralogy and Petrology, v. 112, no. 1, p. 101–118.

Stuiver, Minze, and Reimer, P.J., 1993, Extended ^{14}C data base and revised CALIB 3.0 ^{14}C age calibration program: Radiocarbon, v. 35, no. 1, p. 215–230.

van Wyk de Vries, Benjamin, and Francis, P.W., 1997, Catastrophic collapse at stratovolcanoes induced by gradual volcano spreading: Nature, v. 387, no. 6631, p. 387–390.

Vidal, Nathalie, and Merle, Oliver, 2000, Reactivation of basement faults beneath volcanoes—a new model of flank collapse: Journal of Volcanology and Geothermal Research, v. 99, no. 1–4, p. 9–26.

Voight, Barry, 2000, Structural stability of andesite volcanoes and lava domes: Royal Society of London Philosophical Transactions, v. 358, no. 1770, p. 1663–1703.

Voight, Barry, and Elsworth, Derek, 1997, Failure of volcano slopes: Geotechnique, v. 47, no. 1, p. 1–31.

Voight, Barry, Janda, R.J., Glicken, H.X., and Douglass, P.M., 1983, Nature and mechanics of the Mount St. Helens rockslide-avalanche of 18 May, 1980: Geotechnique, v. 33, no. 1, p. 243–273.

Whittington, C.M., 1996, The petrogenesis of the basalts of Round Head volcano, Kanaga Island, Aleutians: Bloomington, Indiana University, M.Sc. thesis, 79 p.